Tunable RF Photonics Filter using a Comb-based Optical Tapped-Delay-Line with an Optical Nonlinear Multiplexer

Morteza Ziyadi,[1,*] Amirhossein Mohajerin-Ariaei,[1] Mohammad Reza Chitgarha,[1] Salman Khaleghi,[1] Ahmed Almaiman,[1] Yinwen Cao,[1] Amin Abouzaid,[2] Bishara Shamee, [1] Moshe Tur,[3] Loukas Paraschis,[4] Carsten Langrock,[5] Martin M. Fejer,[5] Joseph D. Touch,[2] and Alan E. Willner[1]

[1] *Department of Electrical Engineering, University of Southern California, Los Angeles, California 90089, USA*
[2] *Information Sciences Institute, University of Southern California, 4676 Admiralty Way, Marina del Rey, CA, 90292, USA*
[3] *School of Electrical Engineering, Tel Aviv University, Ramat Aviv 69978, Israel*
[4] *Cisco Systems, 170 W. Tasman Drive, San Jose, California 95134, USA*
[5] *Edward L. Ginzton Laboratory, Stanford University, Stanford, California 94305, USA*
**Corresponding author: ziyadi@usc.edu*

Received Month X, XXXX; revised Month X, XXXX; accepted Month X, XXXX; posted Month X, XXXX (Doc. ID XXXXX); published Month X, XXXX

An RF photonic filter is experimentally demonstrated using an optical tapped delay line based on an optical frequency comb and a PPLN waveguide as multiplexer. The approach is used to implement RF filters with variable bandwidth, shape and center-frequency. ©2014 Optical Society of America

OCIS Codes: (060.2360) Fiber optics links and subsystems; (060.4370) Nonlinear optics, fibers.

Radio frequency (RF) and microwave photonics have many applications due to the low loss and high bandwidth of optical devices and these uses generally require accurate signal filtering and processing [1-3]. These filters are more useful when they can be dynamically reconfigured, tuning their bandwidth, shape, and center frequency using optical signal processing methods [4-5].

Several tunable RF photonic filters have been demonstrated. In one approach, optical filters based on fiber Bragg grating or stimulated Brillouin scattering are used to filter the RF sidebands [6, 7]. In several other approaches, a tapped-delay-line (TDL) structure is used as a key building block to create complex RF photonic filters [8-13]. In the TDL approach, the RF signal is copied into N optical taps that are weighted by coefficients, after which the taps are multiplexed and detected by a photo-diode. This structure employs finite-impulse-response (FIR) filters in the frequency domain. Previous reports have demonstrated tunable tap-based RF filters whose complex tap coefficients can be varied [8-13]. These designs multiplex the tapped signals in the electrical domain following photodetectors [8-13]. Although these approaches produce tunable RF filter functions, they do not easily permit further optical signal processing or transmission since they involve optoelectronic detection.

In this paper, we experimentally demonstrate a variable bandwidth, shape and center-frequency RF photonic filter using a continuously tunable comb-based optical tapped-delay-line (OTDL) with a single optical nonlinear multiplexer and an optical output [14-16]. In [16], we used comb-based OTDL to implement Nyquist filters in the optical domain to generate Nyquist signals. In this paper, we use the similar approach to implement the FIR filters for the application of RF and microwave photonics. Moreover, in this work, tunability and reconfigurability of the approach is studied and experimentally shown. In this approach, the input RF signal is modulated on the frequency lines of an optical frequency comb to create the taps of the OTDL that are delayed by a dispersive element. A periodically poled lithium niobate (PPLN) crystal nonlinearly multiplexes the tapped delay lines in the optical domain to achieve the optical filter output, which then can be used for further optical processes. An electrical filter output can be derived using a photo-diode. The demonstration includes tunable complex coefficient RF filters with different bandwidths of <1 GHz as well as 8-GHz and 32-GHz, as well tunability over the center frequency and different shapes, *e.g.,* Sinc and Gaussian.

The concept of an RF FIR filter using a TDL structure is shown in Fig 1. The input signal is copied onto N paths and each path delayed, and multiplied by an appropriate complex weight. The weighted delayed taps are summed in the time domain, implementing FIR filtering in the frequency domain. Figure 2 depicts an RF photonic filter using a frequency comb-based OTDL. The optical TDL structure requires coherent multiplexing, which is achieved using a mode-locked laser generate the

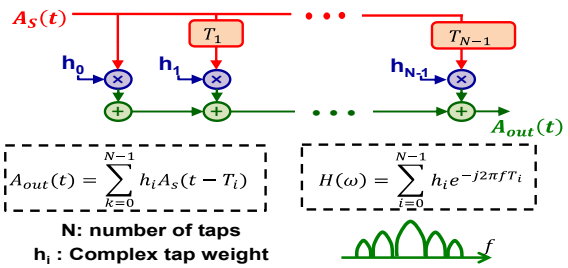

Fig. 1. (Color online) Concept of the FIR filter using a tapped delay line (TDL) structure.

coherent pump components. A programmable phase/amplitude filter, such as a spatial light modulators (SLM) filter based on liquid crystal on silicon (LCoS) technology, separates the frequency lines of the comb source into two paths: the dummy pumps (A_D) and the signals (A_S). The number of frequency components on each path is equal to the number of taps, *i.e.,* N, in the FIR filter. The frequency comb lines of the signal path are modulated with the RF signal, $A_S(t)$, generated by a vector network analyzer (VNA). The result generates N coherent copies of the RF signal on the comb lines. These replicas are sent through a frequency-dependent optical delay element (such as a dispersion compensating fiber (DCF)) to induce signal delays with a relative delay of $\Delta\tau = D\times\Delta\lambda$, where D is the dispersion parameter (ps/nm) and $\Delta\lambda$ is the wavelength separation (nm) between two adjacent frequency lines. Thus T_i in the FIR becomes $T_i=i.\Delta\tau$, $i=0,1,\ldots,(N-1)$. Other RF filters with different bandwidths can be achieved by changing the delay, which this architecture supports by changing the pump-frequency spacing in the comb source or by varying the length of the DCF. The frequency lines of the dummy pumps are sent through the same DCF to increase stability. The delayed signals ($A_{S,i} = A_S(t-i.\Delta\tau)$, $i=0,1,\ldots,(N-1)$) are equivalent to OTDL taps to be coherently combined with the dummy pumps that act as tap weights. A periodically poled lithium niobate (PPLN) waveguide with a quasi-phase matching (QPM) frequency of f_{QPM} multiplexes the taps with the dummy pumps. Tap weights are tuned using the programmable filter to introduce arbitrary phase and amplitude, $A_{F,i}$, on the frequency lines. Inside the PPLN waveguide, in a sum-frequency generation (SFG) process, each replica of the signal $A_{S,i}$ at frequency $f_{S,i}$ combines with a pump $A_{D,i}$ chosen from the dummy pumps group at frequency $f_{D,i}=2f_{QPM}-f_{S,i}$ to generate a new signal at frequency of $f_{D,i}+f_{S,i}=2f_{QPM}$ with a value proportional to $A_{S,i}.A_{D,i}.A_{F,i}$, $i=0,1,\ldots,(N-1)$. Because all signal replicas and dummy pumps are mutually coherent, the resulting signal at $2f_{QPM}$ is the coherent sum of all signals at that frequency. I.e., the signal $\sum_i (A_{S,i}.A_{D,i}.A_{F,i})$ is generated at $2f_{QPM}$. However, because the signal and pumps wavelengths are in C-band, *i.e.,* around 1550 nm, the generated signal will have a wavelength near 750 nm, which cannot propagate in the optical fiber. To convert the generated signal at the second harmonic back to the C-band, another pump laser, A_P, at f_{pump} is injected into the PPLN waveguide using the difference-frequency generation (DFG) process. Thus, the output of the process at $f_{out}=2f_{QPM}-f_{pump}$ is:

$$A_{out}(t) \propto \sum_{i=0}^{N-1} A_P^*.A_{D,i}.A_{F,i}.A_S(t-i\Delta\tau) \quad (1)$$

in which A_P^* is the complex conjugate of the electrical field of the pump. Assuming, $h_i=A^*_P.A_{D,i}.A_{F,i}$, the output becomes;

$$A_{out}(t) \propto \sum_{i=0}^{N-1} h_i A_S(t-i\Delta\tau) \quad (2)$$

which is the FIR filter equation. The resulting FIR filter is a periodic filter with a free spectral range (FSR) of $1/\Delta\tau$ which can be tuned by varying relative delay. The desired filtering at the output could be achieved by adjusting the phase and amplitude of the coherent pumps to the tap weights of the FIR filter. The output of the designed FIR filter can be either (a) kept in the optical domain or (b) transferred to the RF domain using a photodiode, whose electrical output can be analyzed in the VNA. Keeping the signal in the optical domain enables further optical processing of the RF signal.

Figure 3 shows the experimental setup for the RF photonic filter using a comb-based OTDL. A mode-locked laser with a 10GHz repetition rate and 2-ps pulse width generates a coherent frequency comb, which passes through a delay line interferometer (DLI) with a free spectral range (FSR) of 20-GHz to increase its frequency spacing. The resulting 20-GHz frequency comb is sent through an erbium-doped fiber amplifier (EDFA) and a highly nonlinear fiber (HNLF) to generate a flat and broad spectrum (as shown in the figure). A programmable phase and amplitude filter based on liquid crystal on silicon

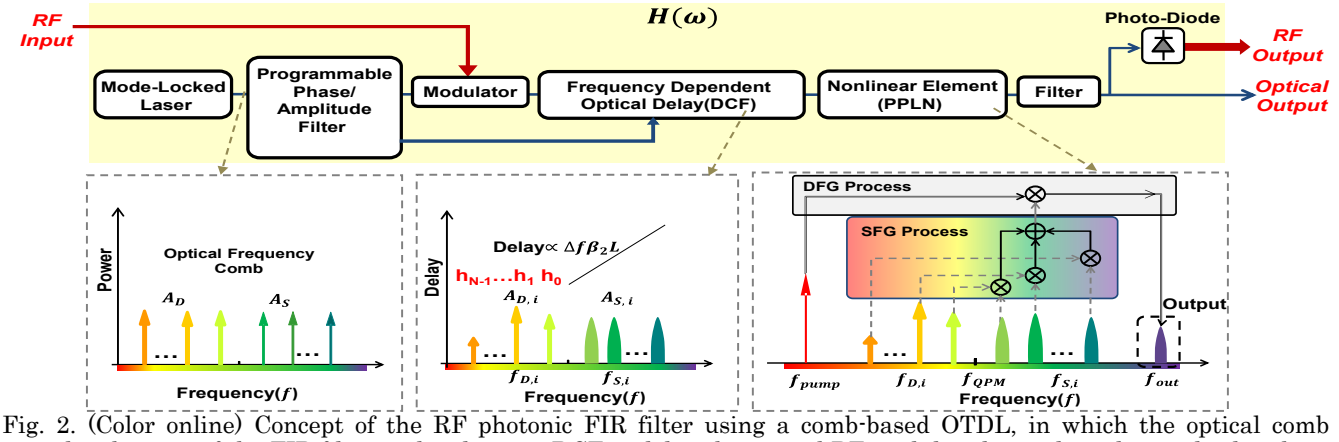

Fig. 2. (Color online) Concept of the RF photonic FIR filter using a comb-based OTDL, in which the optical comb provides the taps of the FIR filter and utilizing a DCF to delay the tapped RF modulated signals and to multiplex them in a PPLN.

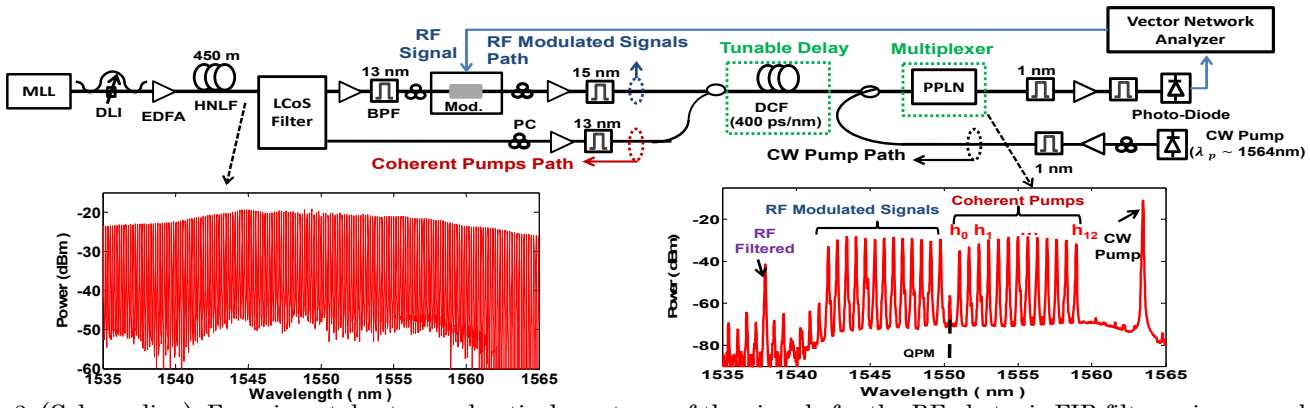

Fig. 3. (Color online) Experimental setup and optical spectrum of the signals for the RF photonic FIR filter using a comb-based OTDL. BPF: Band Pass Filter; PC: Polarization Controller.

(LCoS) technology is used to select and write complex weights on the frequency comb lines, and to separate the lines into two paths: the signals and the coherent pumps. For each path, up to 13 comb lines are selected with a frequency spacing of 80-GHz (0.64 nm). In the signal path, after pre-amplification in an intensity modulator, an RF signal is generated by a vector network analyzer (VNA) is modulated on the frequency lines. After sufficient EDFA amplification, the signals and pumps travel through a DCF to introduce relative delays on the signals that act as a delay line in the FIR filter. With another amplified continuous wave (CW) laser pump at ~1564 nm, all the signals and pumps are sent into a 4-cm-long PPLN waveguide with a temperature-tuned QPM wavelength of ~1550.5 nm which is the middle point of the selected comb lines to create the photonic RF FIR filter with the optical spectrum shown in the figure. It should be mentioned that the rate of change in phase-matching of the PPLN waveguide is 0.13 nm/degree C and in our experiment the variations of ±0.5 degree C does not have too much effect. However, high QPM detuning would cause less conversion efficiency corresponds to the less performance of the system. The output signal is filtered and sent to a photo-diode to be analyzed in the VNA.

The tap weights, h_i's, must be calibrated to tune the RF filter properties such as shape, bandwidth, etc. The calibration process is similar to the approach that presented in [16]. The tap weights are calibrated to the appropriate values, with the central tap selected as the reference tap. In order to calibrate the tap-k coefficient, the coefficients are set as $h_i=1$ for the reference tap and tap-k and $h_i=0$ for the rest of the taps. The corresponding pump is disabled to set a coefficient to 0. To tune a coefficient to 1, the amplitude and phase of the corresponding pump are tuned in the LCoS filter to achieve a symmetric shape at the output spectrum. In fact, complex coefficients are tuned by LCoS filter to implement the calibration process. After calibrating all the taps, the amplitude and phase of the taps are adjusted to the tap weights of the desired FIR filter.

Figures 4 (a), (b) and (c) show experimental and simulated results using a DCF with dispersion parameter of 80 ps/nm which generates a FIR filter with an FSR of ~ 20 GHz. Nine frequency lines implement a nine-tap FIR filter in which the amplitude and phase of the taps is tuned to achieve different shapes and bandwidths (BWs). The experimental result is similar to the simulated design. Filters with BWs of <1 GHz and ~3 GHz can be implemented. Moreover, different ratios of the main lobe to the side lobe of 10-20 dB are measured. This approach is the same as a TDL implementation in the RF domain using optical waves. Thus, after calibration, tap coefficients are the same as in the simulation, which facilitates tuning the filter properties. The FSR of the filter can be tuned to 12 GHz by replacing the DCF with one supporting ~ 130 ps/nm, the result of which is shown in Fig. 4(d). Using a ~ 400 ps/nm DCF can achieve a filter with an FSR of 4 GHz, as shown in Figs. 5 (a)-(d). RF

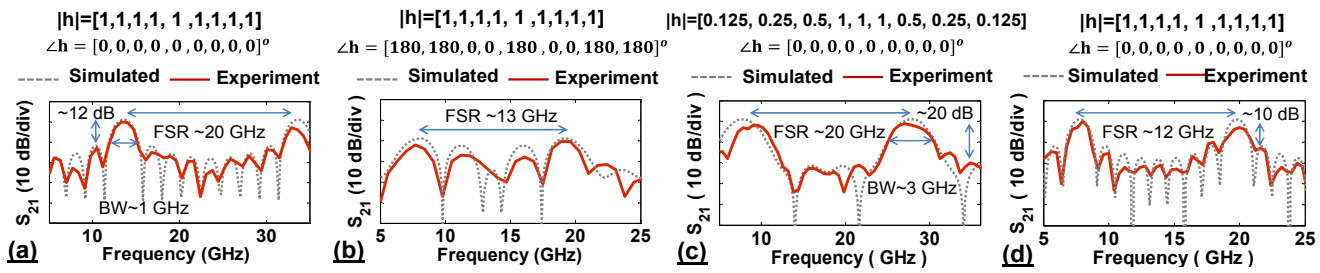

Fig. 4. (Color online) Experimental results for 9-tap FIR RF photonic filters with (a), (b), (c) showing an FSR of 20 GHz using an 80 ps/nm DCF. The tap coefficients (h) are tuned in both phase and amplitude to implement different filters. (d) An FSR of 12 GHz using 130-ps/nm DCF. Experimental results match the simulated design.

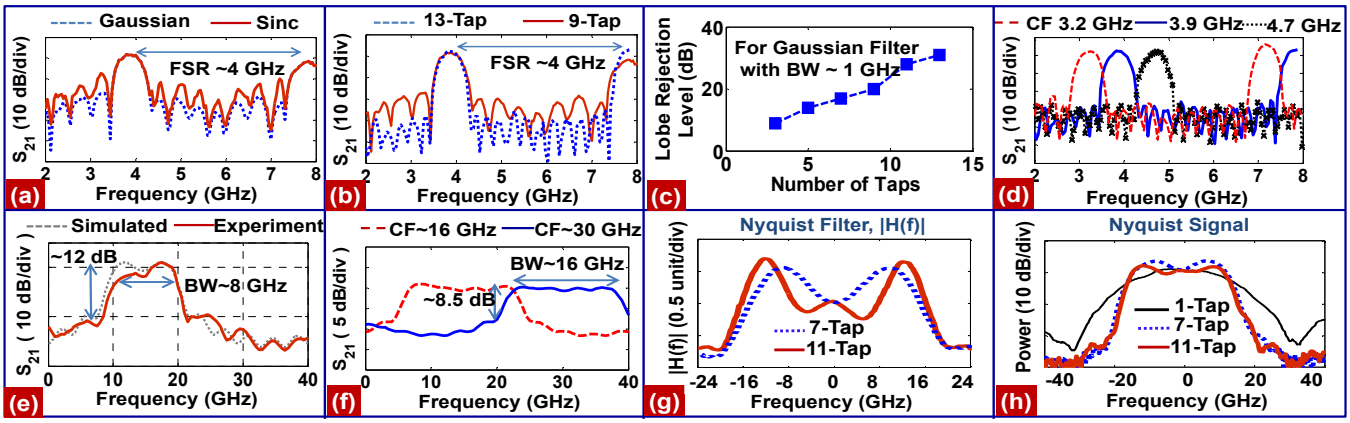

Fig. 5. (Color online) Experimental results: (a) Different shapes for a 9-tap FIR filter with an FSR of 4-GHz using a 400 ps/nm DCF, (b) Tunability over the number of taps, (c) Measured lobe rejection level for the filters of part (b), (d) Tunability over the central frequency, (e) An FIR filter with a BW of 8-GHz using a 40 ps/nm DCF, (f) A tunable FIR filter with BW of 16-GHz (g) Nyquist filter with a BW of 32-GHz, (h) Generated optical Nyquist signal.

filters with different number of taps and shapes can also be implemented (Figs. 5(a) and (b)). For the Sinc (*Sinc(x)=sin(x)/x*) shape, the taps all have the same coefficient. As shown in Fig. 5(c), increasing the number of taps achieves filters with a high value of lobe rejection level measured as a ratio of the main lobe to the side lobes. Achieving filters with different shapes and bandwidth and lobe rejection levels shows the reconfigurability of the approach.

The ability to implement complex coefficients allows us to tune the center-frequency (CF) of the filter as shown in Fig. 5(d). Slight variation of phase on the tap coefficients which is equivalent to frequency shift, is utilized to tune the CF of the filter [15]. This could be implemented by choosing complex tap coefficients in the LCoS filter. For instance, in Fig. 5 (d), the taps of the filter at CF of 3.9 GHz have phase values of [0, -60,-120,170,100,45, -20,-80,-140,150,90]° compared to the filter at CF of 3.2 GHz.

This approach can also implement very broad band filters. To achieve a broad band filter with the range of several GHz, the tap delay time is changed by varying either the wavelength spacing of the frequency comb lines or the length of the DCF. Figure 5(e) illustrates how use of a 40 ps/nm DCF can implement a filter with an FSR of 40-GHz and bandwidth of ~ 8-GHz. By reconfiguring the tap coefficients, filters with the BW of 16 GHz and different CFs are implemented (Fig. 5(f)). Frequency lines with a spacing of 120 GHz (0.965 nm) and a 16 ps/nm DCF can implement Nyquist filters with the BW of 32-GHz to generate optical Nyquist data channels at 32 Gbaud (Fig. 5 (g), (h)). Tunability of these broad band filters are demonstrated by implementing Nyquist filters at 26-GHz bandwidth, as shown in [16]. In conclusion, FIR RF photonic filters can be generated with complex coefficients. Tunable FIR filters with a wide range of parameters can be achieved using a comb-based OTDL in a single PPLN waveguide. By implementing the FIR filter in the time domain using an OTDL enables further optical processing of the filtered RF signal.

This work was made possible by the support from the NSF and the Center for Integrated Access Networks.

References

1. J. Capmany, B. Ortega, and D. Pastor, J. Lightw. Technol., **24**(1), 201–229 (2006).
2. R. A. Minasian, IEEE Trans. Microw. Theory Tech., **54**(2), 832–846, Feb. (2006).
3. A. J. Seeds, and K. J. Williams, J. Lightw. Technol. **24**, 4628–4641 (2006).
4. J. Yao, J. Lightw. Technol. **27**, 314-335 (2009).
5. J. Capmany, J. Mora, I. Gasulla, and J. Sancho, J. Lightw. Technol., **31**(4), pp. 571–586 (2013).
6. J. Palac´ı, P. Perez-Millan, G. E. Villanueva, J. L. Cruz, M. V. Andr´es, J. Mart´ı, and B. Vidal, IEEE Photon. Technol. Lett., **22**(19), pp. 1467–1469 (2010).
7. W. Zhang and R. A. Minasian, IEEE Photon. Technol. Lett., **23**(23), 1775–1777 (2011).
8. V. R. Supradeepa, C. M. Long, R. Wu, F. Ferdous, E. Hamidi, D. E. Leaird, and A. M. Weiner, Nature Photon., **6**, 186–194 (2012).
9. X. Xue, X. Zheng, H. Zhang, and B. Zhou, J. Lightw. Technol., **31**(13), 2263– 2270 (2013).
10. L. Li, X. Yi, T. X. H. Huang, and R. A. Minasian, Opt. Express, **20**(10), 11517–11528 (2012).
11. A. Ortigosa-Blanch, J. Mora, J. Capmany, B. Ortega, and D. Pastor, Opt. Lett., **31**(6), 709–711 (2006).
12. X. Xue, Y. Xuan, H.-J. Kim, J. Wang, D. E. Leaird, M. Qi, and A. M. Weiner, J. Lightw. Technol. **32**, 3557-3565 (2014).
13. H.-J. Kim, D. E. Leaird, A. J. Metcalf, and A. M. Weiner, J. Lightw. Technol. **32**, 3478-3488 (2014)
14. M. Ziyadi, M. R. Chitgarha, S. Khaleghi, A. Mohajerin-Ariaei, A. Almaiman, J. Touch, M. Tur, C. Langrock, M. M. Fejer, and A. E. Willner, Opt. Express **22**, 84-89 (2014).
15. M. Ziyadi, A. Mohajerin-Ariaei, M. Chitgarha, S. Khaleghi, A. Almaiman, A. Abouzaid, J. Touch, M. Tur, L. Paraschis, C. Langrock, M. M. Fejer, and A. Willner, in CLEO: 2014, OSA Technical Digest (online) (Optical Society of America, 2014), paper STu3I.4.
16. M. Ziyadi, M. R. Chitgarha, A. Mohajerin Ariaei, S. Khaleghi, A. Almaiman, Y. Cao, M. J. Willner, M. Tur, L. Paraschis, C. Langrock, M. M. Fejer, J. D. Touch and A. E. Willner, Opt. Lett. **39**, 6585-6588 (2014).

References (Long Format)

1. J. Capmany, B. Ortega, and D. Pastor, "A tutorial on microwave photonic filters," J. Lightw. Technol., **24**(1), 201–229 (2006).
2. R. A. Minasian, "Photonic signal processing of microwave signals," IEEE Trans. Microw. Theory Tech., **54**(2), 832–846, Feb. (2006).
3. A. J. Seeds, and K. J. Williams, "Microwave photonics." J. Lightw. Technol. **24**, 4628–4641 (2006).
4. J. Yao, "Microwave Photonics," J. Lightw. Technol. **27**, 314-335 (2009).
5. J. Capmany, J. Mora, I. Gasulla, and J. Sancho, "Microwave photonic signal processing," J. Lightw. Technol., **31**(4), pp. 571–586 (2013).
6. J. Palac´ı, P. Perez-Millan, G. E. Villanueva, J. L. Cruz, M. V. Andr´es, J. Mart´ı, and B. Vidal, "Tunable photonic microwave filter with single bandpass based on a phase-shifted fiber Bragg grating," IEEE Photon. Technol. Lett., **22**(19), pp. 1467–1469 (2010).
7. W. Zhang and R. A. Minasian, "Widely tunable single-passband microwave photonic filter based on stimulated Brillouin scattering," IEEE Photon. Technol. Lett., **23**(23), 1775–1777 (2011).
8. V. R. Supradeepa, C. M. Long, R. Wu, F. Ferdous, E. Hamidi, D. E. Leaird, and A. M. Weiner, "Comb-based radiofrequency photonic filters with rapid tunability and high selectivity," Nature Photon., **6**, 186–194 (2012).
9. X. Xue, X. Zheng, H. Zhang, and B. Zhou, "Analysis and compensation of third-order dispersion induced RF distortions in highly reconfigurable microwave photonic filters," J. Lightw. Technol., **31**(13), 2263– 2270 (2013).
10. L. Li, X. Yi, T. X. H. Huang, and R. A. Minasian, "Distortion-free spectrum sliced microwave photonic signal processor: Analysis, design and implementation," Opt. Express, **20**(10), 11517–11528 (2012).
11. A. Ortigosa-Blanch, J. Mora, J. Capmany, B. Ortega, and D. Pastor, "Tunable radio-frequency photonic filter based on an actively mode-locked fiber laser," Opt. Lett., **31**(6), 709–711 (2006).
12. X. Xue, Y. Xuan, H.-J. Kim, J. Wang, D. E. Leaird, M. Qi, and A. M. Weiner, "Programmable Single-Bandpass Photonic RF Filter Based on Kerr Comb from a Microring," J. Lightw. Technol. **32**, 3557-3565 (2014).
13. H.-J. Kim, D. E. Leaird, A. J. Metcalf, and A. M. Weiner, "Comb-Based RF Photonic Filters Based on Interferometric Configuration and Balanced Detection," J. Lightw. Technol. **32**, 3478-3488 (2014)
14. M. Ziyadi, M. R. Chitgarha, S. Khaleghi, A. Mohajerin-Ariaei, A. Almaiman, J. Touch, M. Tur, C. Langrock, M. M. Fejer, and A. E. Willner, "Tunable optical correlator using an optical frequency comb and a nonlinear multiplexer," Opt. Express **22**, 84-89 (2014).
15. M. Ziyadi, A. Mohajerin-Ariaei, M. Chitgarha, S. Khaleghi, A. Almaiman, A. Abouzaid, J. Touch, M. Tur, L. Paraschis, C. Langrock, M. M. Fejer, and A. Willner, "Experimental Demonstration of a Variable Bandwidth, Shape and Center-Frequency RF Photonics Filter using a Continuously Tunable Optical Tapped-Delay-Line and Having an Optical Output," in CLEO: 2014, OSA Technical Digest (online) (Optical Society of America, 2014), paper STu3I.4.
16. M. Ziyadi, M. R. Chitgarha, A. Mohajerin Ariaei, S. Khaleghi, A. Almaiman, Y. Cao, M. J. Willner, M. Tur, L. Paraschis, C. Langrock, M. M. Fejer, J. D. Touch and A. E. Willner, "Optical Nyquist channel generation using a comb-based tunable optical tapped-delay-line," Opt. Lett. **39**, 6585-6588 (2014).